A two-stage power converter architecture with maximum power extraction for low-power energy sources

Ridvan UMAZ[*]

Technical Vocational School, Bitlis Eren University, Bitlis, Turkey

Abstract: A two-stage power converter with maximum power extraction for energy harvesting is presented. The power converter consists of two stages; a maximum power extraction stage (i.e. first stage) and a regulation stage (i.e. second stage). The first stage consists of a number of charge pumps connected in parallel to extract power from the energy source while the second stage steps up low input voltage level to a usable level for a load. Proposed converter operates as low as 0.3 V and the output up-converts to 3.3 V. The proposed converter is aimed to extract maximum power from either low-power energy sources or high-power energy sources without increasing the complexity of the converter. Measured results indicate that the tracking efficiency is enhanced by 117%–123% over a single charge pump in the first stage converter. Proposed power converter provides 66.7% more power extracted from the energy source than the single charge pump one. The end-to-end efficiency is enhanced by $1.67\,X$ as compared to the single charge pump implementation.

Key words: Power converter, boost converter, charge pump, energy harvesting, maximum power

1. Introduction

Energy harvesting uses the surrounding environmental energy sources to supply power to an extensive set of applications, such as wireless sensor networks and remote devices [1, 2]. Photovoltaic cells [3], thermoelectric generators (TEGs) [4], piezoelectronics [5], RF [6], and microbial fuel cells (MFCs) [7] as deploying energy sources are available for harvesters to utilize at various loads.

Energy sources generally generate low voltage and power at their outputs (i.e. in the range of mV and μW) [8–10]. Since energy harvesting initiates with low ambient voltage levels, the generated voltages from energy sources are normally low, ranging from tens of millivolts to hundreds of millivolts. However, these voltage levels are inadequate for electronic devices (e.g., sensors) to operate properly. In addition, energy sources are not well suited to directly power up electronic devices, because the voltage levels at the outputs of energy sources can fluctuate considerably during operation. Hence, designing a low input voltage (e.g., less than 1 V) power converter is essential to step up the low voltage to a usable level by the load, as shown in Figure 1.

Mainly two types of power converters are available; one-stage (see Figure 1a) and two-stage (see Figure 1b) converters. One-stage converters up-convert the output voltage to a level required by the load is implemented with a single converter. It also extracts maximum power from energy sources at the single converter if desired.

However, two-stage converters consist of two converters. The first stage is used to both boost the low input voltage to a sufficient level for the second one to operate and to extract maximum power from energy sources, whereas second one is deployed to regulate output voltage from an intermediate storage element to

*Correspondence: ridvanumaz@gmail.com

a stable supply voltage (e.g., 3.3 V) for loads. In Figure 1b, the energy extracted from the sources needs to be accumulated over time and intermittently transferred to loads due to inherently low voltage and power at the outputs of the sources. A super capacitor as an intermediate storage element at V_{cp} is used to efficiently accumulate energy.
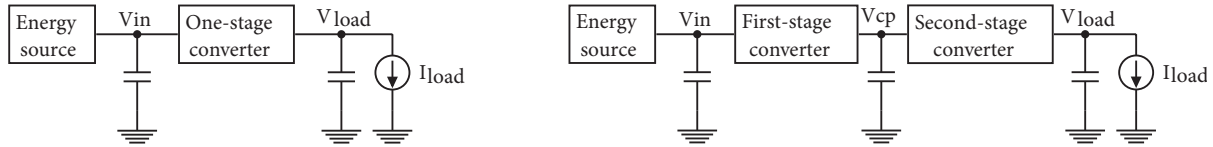

Figure 1. (a) The block diagram of a one-stage power converter. (b) The block diagram of a two-stage power converter.

Conventional one-stage [19] and two-stage [7, 17] power converters do not consider maximum power extraction from energy sources, but the harvesters need to be established efficiently to reach maximum power extraction. By adjusting system parameters (e.g., number of stages in charge pump, switching frequency, and duty cycle), the maximum power available from the energy sources can be achieved. However, it requires either to get help of digital signal processing or central processing unit, or to implement some power-consuming control logic circuitry in order to adjust these system parameters. For example, two different microbial fuel cells (MFCs) used as energy sources [11] produce a maximum power of 11.2 μW (MFC-Low) and 1.6 mW (MFC-High), and a maximum power extraction circuit is implemented in order to attain this. However, the circuit consumes the peak power of 36.4 μW which is much higher than the MFC-Low power output. Thus, this maximum power extraction circuit is not appropriate for all energy sources. For low energy sources, maximum power extraction circuits should be ultralow-power as well as be designed for a variety of power ranges in energy sources.

In order to maximize power extraction for a variety of power ranges in energy sources, this paper develops an efficient two-stage power converter for renewable energy sources without introducing additional power overhead and circuit complexity. The first stage utilizes a number of off-the-shelf charge pumps connected in parallel to maximize the power extraction from energy sources. The second stage is a commercial boost converter which steps up the output voltage at the required level by the load. Instead of needing external sources such as a battery or complex circuits, the proposed converter achieves maximum power output from low-power energy sources due to multiple charge pumps. In comparison with a single charge pump implementation in the first stage converter, the proposed converter with five charge pumps indicates some distinct advantages: (1) the maximum power extraction from energy sources is enhanced by 117%–123% over single one; (2) 66.7% more end-to-end efficiency is obtained.

The rest of the paper is organized as follows. Section 2 discusses the design considerations for one and two-stage power converters. Section 3 describes how to achieve maximum power extraction. In Section 4, proposed two-stage power converter is presented and its circuit implementation is given. Experimental results and evaluation are provided in Section 5 and the conclusions are drawn in Section 6.

2. Design consideration

Energy harvesting circuits can be based upon either one- or two-stage power converter, as shown in Figure 1. Mainly two types of one-stage power converters are available; charge pump (capacitive) and boost converter (inductive). In energy harvesting systems, capacitive power converters can be principally used as either a step-up power converter [12] or an auxiliary circuit (e.g., start-up) [13]. Compared to an inductive boost converter, which is most of the time an essential part in energy harvesting system, capacitive one comes fully integrated

Table 1. Summary of power converters.

	Circuit	Pros	Cons
One-stage	Charge pump	Low Vin & integrated Self-start-up ability Energy processed once	Low Vout Low efficiency
	Boost converter	High Vout High efficiency Energy processed once	High Vin Off-chip inductor
Two-stage	Charge pump + Boost converter	Low Vin High Vout Self-start-up ability	Off-chip inductor Energy processed twice Low efficiency

on a chip with better self-start-up ability, and operates at a low voltage level and is thus more applicable for low-power energy harvesting systems. However, the capacitive one is well-known to achieve low conversion efficiency and output voltage. Moreover, it does not provide a sufficient voltage level to some load applications (e.g., 3.3 V) and even if it does, it provides low power efficiency which does not power up the load.

Although one-stage power converters provide some advantages with the implementation of either capacitive (i.e. charge pump) or inductive types in volume-constrained low-power energy harvesting systems, there are some issues inherent to such circuits, such as self-start-up ability and high voltage at the output. A solution to these issues is to incorporate capacitive and inductive into a single system which is called two-stage power converter, as shown in Figure 1.This combines the capacitive ones' ability to provide better self-start-up with the inductive ones' high voltage output. To compare with one-stage power converters, two-stage ones process the harvested energy twice with different efficiency rates before powering the load due to the two converters in series. Thus, the overall efficiency is constrained. The overall efficiency (η_{two}) of the energy harvesting circuit is a product of efficiency of the first stage converter i.e. charge pump (η_{cp}) and the second-stage converter i.e. boost converter (η_{dc}), and expressed as

$$\eta_{two} = \eta_{cp} \times \eta_{dc}, \tag{1}$$

The efficiencies comparison is expressed as

$$\eta_{two} < \eta_{one}$$
$$\eta_{two} < \eta_{cp} < \eta_{dc} \tag{2}$$

Comparison of power converters for some parameters are summarized in Table 1. Two-stage power converter architecture operates in low voltage and up-converts to high voltage without need of external source to start-up. These achievements are superior to one-stage power converter i.e. not achieved all these in either charge pump or boost converter.

3. Maximum power extraction

In order to present energy sources' internal equivalent circuits, electrical models which are varied for each energy source are used. TEGs, MFCs and GBFCs (Glucose biofuel cells) can be modeled as a voltage source in series with a resistor while solar cells can be modeled as a current source in parallel with a diode. However, all energy sources can be generally modeled as the Th$\acute{e}$venin equivalent circuit which includes a Th$\acute{e}$venin voltage in series
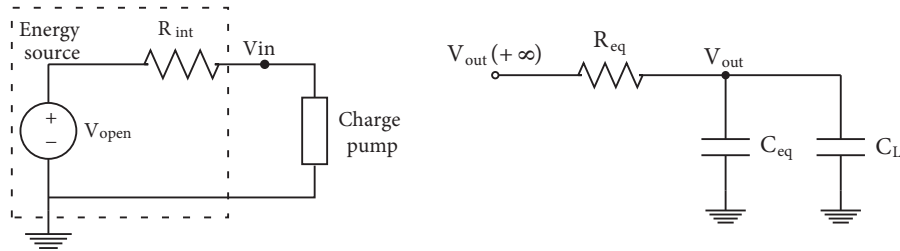
Figure 2. (a) Th$é$venin electrical equivalent circuit for energy sources (e.g. GBFCs, solar cells, MFCs, TEGs). (b) The equivalent circuit of the charge pump.
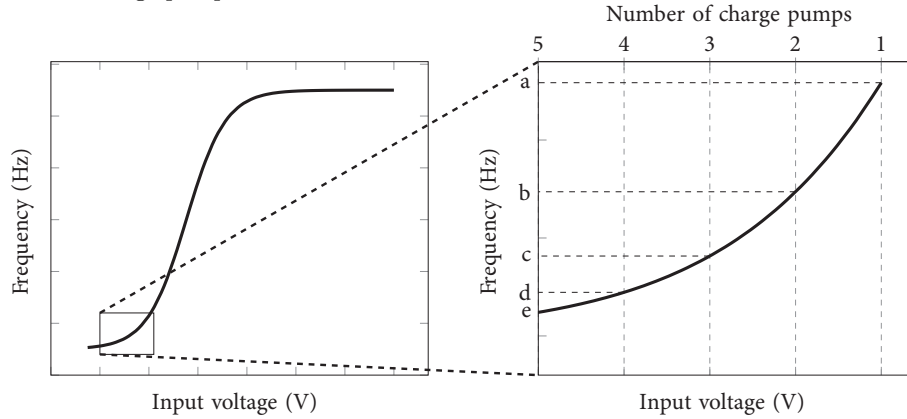

Figure 3. Input voltage Vin vs frequency f. Zoomed area of left figure illustrates number of charge pump vs f.

with a Th$é$venin equivalent impedance including resistance, capacitance and inductance. Figure 2a shows the Th$é$venin equivalent circuit for energy sources (e.g. GBFCs, solar cells, TEGs and MFCs) with a charge pump (i.e. first stage converter) connected in parallel.

Maximum power extraction from an energy source is achieved when the input impedance (R_{eq}) of the connected devices (e.g. resistive loads, charge pumps, boost converters or others) interfacing with the source is examined to be equal to the source internal impedance (R_{int}). This is referred as the impedance matching theory and represented as $R_{int}=R_{eq}$.

According to the theory, the maximum power can be represented as

$$P_{max} = \frac{V_{open}^2}{4R_{int}}. \tag{3}$$

Figure 2b shows the equivalent circuit of the charge pump. In this figure, $V_{out}(+\infty)$ is the output voltage in the steady state and is given by [14]

$$V_{out}(+\infty) = (N+1) \times Vin. \tag{4}$$

The output impedance of the charge pump is given by [15]:

$$R_{eq} = \frac{N}{f \times C}, \tag{5}$$

where N is the number of stages, f is the switching frequency, and C is the pumping capacitor.

It is seen that the impedance can be adjusted by setting either the number of stages or the switching frequency.

As an off-the-shelf charge pump (Seiko S-882) [16] is used in this work, the number of stages is fixed and thus is not a design parameter to extract maximum power from energy sources. In [16], input voltage Vin versus the switching frequency f is shown at left side of Figure 3. This figure shows how the switching frequency changes with a varying input voltage. Discrete charge pump S-882 has a larger output impedance than energy sources [7, 17]. Thus, input voltage is far from the voltage at the maximum power point. There is no way to adjust the switching frequency of the off-the-shelf charge pump to extract maximum power from energy sources due to unavailability of a frequency control pin on the pump. A simple way should be by decreasing input voltage with increasing the number of deployed charge pumps at the first stage, as shown in Figure 4. Once a number of charge pumps are deployed, the switching frequencies of the charge pumps decrease with a decreasing input voltage, as shown in the right side of Figure 3.

The impedance for one charge pump at the frequency of a is given by

$$R_{eq}(1) = \frac{N}{a \times C} \tag{6}$$

Once two pumps connected in parallel are employed in Figure 4, the impedance for each charge pump at the frequency of b is given by

$$R_{eq}(2) = \frac{N}{b \times C} = \frac{R_{eq}(1) \times a}{b}, \tag{7a}$$

and equivalent impedance is expressed as

$$R(2)_{EQ} = \frac{R_{eq}(1) \times a}{2 \times b} \tag{7b}$$

Continuing the process, the general forms for n charge pumps are expressed as

$$R_{eq}(n) = \frac{R_{eq}(1) \times f(1)}{f(n)}, \tag{8a}$$

$$R(n)_{EQ} = \frac{R_{eq}(1) \times f(1)}{n \times f(n)}. \tag{8b}$$

The frequency and the impedance comparisons are expressed as

$$f(1) > f(2) > ... > f(n), \tag{9a}$$

$$R_{eq}(1) < R_{eq}(2) < ... < R_{eq}(n), \tag{9b}$$

$$R(1)_{EQ} > R(2)_{EQ} > ... > R(n)_{EQ}. \tag{9c}$$

Assuming $f(1) \approx f(n)$, the equivalent impedance for n charge pumps in Figure 4 is assumed linearly reciprocal to the number of the pumps and expressed as

$$R_{lin}(n)_{EQ} = \frac{R_{eq}(1)}{n} = \frac{Z_L}{n}. \tag{10}$$

However, according to the right image of Figure 3, the equivalent impedance is exponentially reciprocal to the number of the pumps (see (8)). The difference between (8) and (10) (i.e. mismatch) is then expressed as

$$\Delta R = \frac{R_{eq}(1)}{n} \times \left(\frac{f(1)}{f(n)} - 1 \right). \tag{11}$$

Note that for simplicity and unknown structure of S-882 charge pump (i.e. oscillator circuit and charge pump stages) and switching frequencies for each number of pump once connected in parallel, (10) is used for the equivalent impedance with n first stage converters to calculate tracking efficiency. For this study, the impedance mismatch in (11) results in less than 7.5% high tracking efficiency. This will be discussed in detail in Section 5.
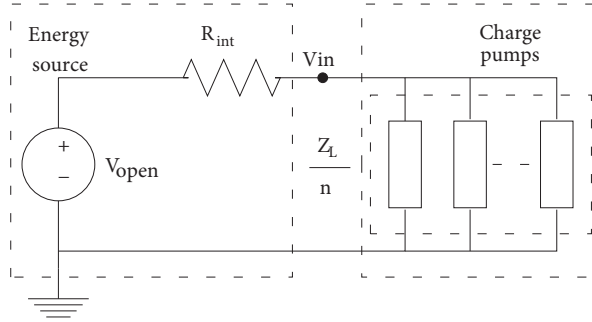

Figure 4. Thevenin electrical equivalent circuit for energy sources with n charge pumps connected in parallel.
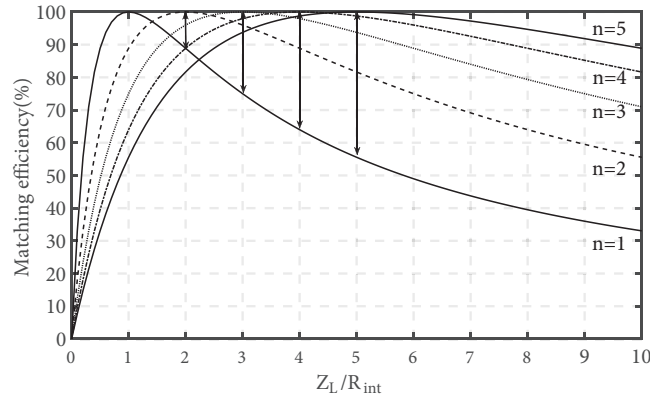

Figure 5. Matching efficiency η_{track} as a function of Z_L/R_{int} with varying the number of charge pumps.

In Figure 4, the power delivered to the n charge pumps connected in parallel can be described as

$$P_L = (\frac{V_{open}}{R_{int} + \frac{Z_L}{n}})^2 \times \frac{Z_L}{n} \tag{12}$$

The matching efficiency η_{track} can be viewed as the ratio of P_L to P_{max}, given by

$$\eta_{track} = \frac{P_L}{P_{max}} = \frac{4}{\frac{Z_L}{n \times R_{int}} + \frac{n \times R_{int}}{Z_L} + 2}. \tag{13}$$

Figure 5 shows the matching efficiency as a function of Z_L/R_{int} with varying the number of charge pumps (n). In order to extract more than 90% of the available power from the energy sources, the tolerable impedance mismatch ranges from –48% to +93% for one charge pump. This range can be proportionally extended with the number of the charge pumps connected in parallel. This indicates that the number of charge pumps (n) has a significant error endurance over one charge pump in the design. Thus, the power at the output stands very close to the maximum power point (MPP) even once a large impedance mismatch occurs in the proposed converter design. Instead of employing more complex power-hungry peripheral circuits as in conventional MPP designs, this is a simple and self-starting method to obtain maximum power extraction from energy sources.

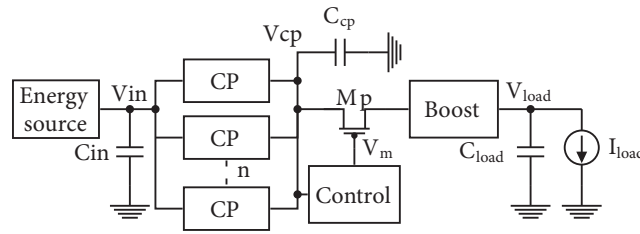## 4. Proposed two-stage power converter

Figure 6. Proposed two-stage power converter.

Figure 6 shows the block diagram of the proposed two-stage power converter architecture including a power extraction unit (i.e. first stage converter), an intermediate storage element C_{cp}, a switch control circuit, and a boost converter (i.e. second-stage converter). The power extraction unit consists of n number of charge pumps connected in parallel which achieve approaching the maximum power point. The input voltage of the power converter Vin is decreased through this connection to approach closely to a voltage level at maximum power point. This is mainly due to the fact that the switching frequencies of the pumps are decreased and the equivalent impedance of the power extraction unit is matched with the energy source one. The charge pump S-882 from Seiko Instruments [16] was used. It requires an input voltage as low as 0.3 V and can charge to 2 V and discharge to 1.44 V. Each charge pump needs a local capacitor to first accumulate the energy harvested from the energy source. Once all charge pumps concurrently charge to its discharge start voltage (2V), the stored energy at their local capacitors are released through the outputs of the charge pumps to a second storage element (i.e. super capacitor).

The implementation of the power extraction unit requires n number of local capacitors and one super capacitor. Local capacitors are initially charged and then the stored charge is transferred to the super capacitor to charge, i.e. two charging processes are carried out. This implementation leads to a large area overhead and energy losses.

A more efficient implementation uses one super capacitor as the intermediate storage element instead of employing individual local capacitors for each charge pump and the second storage element. This shared super capacitor for n number of charge pumps results in savings of (n-1) local capacitors, one second storage element and one charging process. Since the component count decreases, the proposed design is efficient from a size, cost, and energy loss perspective. Using the shared-capacitor C_{cp} introduces new design considerations on the design of the power extraction unit. Characteristically, the shared-capacitor needs newly designed charge start and discharge voltage levels to deliver the stored energy to second-stage converter (i.e. boost converter). For this study, discharge start voltage is decreased from 2 V to 1.5 V and charge start voltage is lowered from 1.44 V to 1.06 V. This functionality is obtained through a control circuit, as shown in Figure 7.

The switch PMOS transistor Mp interfaces between the shared-capacitor and the boost converter. The PMOS transistor is controlled by the control circuit to manage energy accumulation and transfer processes.

A brief operation of the control circuit is that the voltage across the super capacitor goes through diodes and the N1 NMOS transistor and reach the gate of N2 NMOS transistor. Once enough voltage appears at the gate of N1 transistor, i.e. exceeds the threshold voltage of N2 transistor, ground (e.g., source of N2 transistor) connects to V_m and turns on M_p PMOS. The stored energy at the super capacitor is transferred to the boost converter. Once the super capacitor discharge to the level whose voltage is not sufficient to keep the N2 transistor turning on, the N2 transistor is cut off and the M_p PMOS transistor is deactivated. The energy transferring

from the super capacitor to the boost converter is cut off. This process repeats over the time. A more detailed explanation of the control circuit is provided in [7].

The values for the discharge start and charge start voltages can be easily expanded at the expense of few extra components. The requirement of specific applications (e.g., power requirement for a load) is important in the selection of the shared-capacitor. For the purpose of demonstration, a super capacitor of 50.94 mF is used.
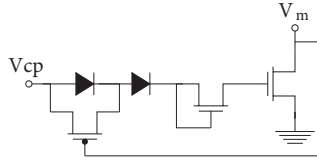

Figure 7. Control circuit for transferring stored energy at V_{cp} to second-stage converter [7].

As second-stage converter, the boost converter L6920DB from ST microelectronics [18] is used to up-convert low voltage at Vcp to a high voltage level (i.e. 3.3 V) at V_{load} for the load.

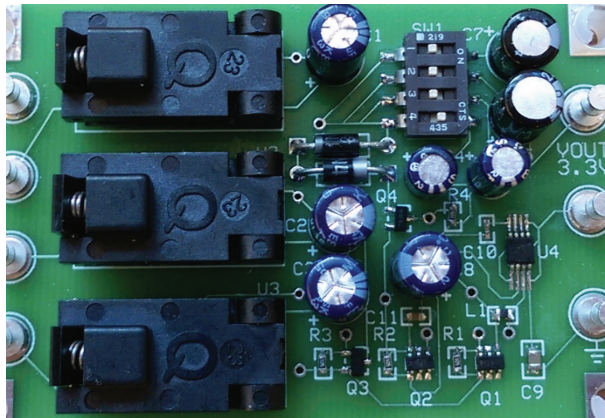The fabricated PCB of the proposed power converter is shown in Figure 9.

Figure 8. PCB implementation of the proposed power converter.

5. Measurement results

A test circuit using off-the-shelf components was constructed to measure the effectiveness of the proposed two-stage power converter with maximizing power extraction from the energy source. A 750 mV input voltage source in series with a 1 kΩ internal resistor was used to emulate the energy source.

In order to evaluate power extraction from the energy source, the number of charge pumps are varied from 1 to 5 in the proposed power converter. For demonstration purposes, Figure 10 shows three charge pumps and the voltage levels at the input of the converter are monitored with different numbers of the pumps. The input voltage decreases as the number of the pumps increases. Thus, the voltage approaches very close to the voltage level at the maximum power point.

Figure 11 shows measured tracking efficiency and the stored energy at the shared-capacitor under varying number of charge pumps. The stored energy P_{cp} at the element is calculated as

$$P_{cp} = (1/2t) \times C \times (V_d^2 - V_c^2), \tag{14}$$

where V_c is the charge start voltage and V_d is the discharge start voltage. t is the time for the shared-capacitor C_{cp} to charge from V_c to V_d.

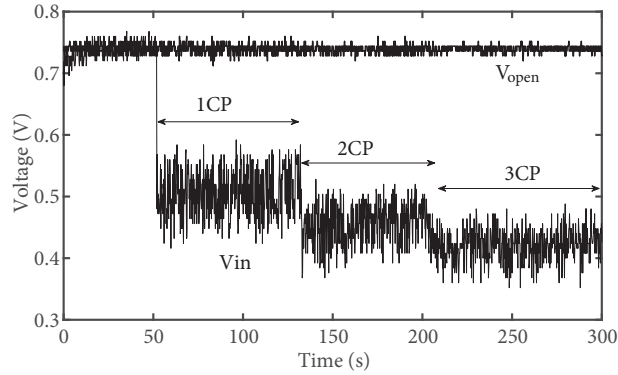**Figure 9**. PCB implementation of the proposed power converter.

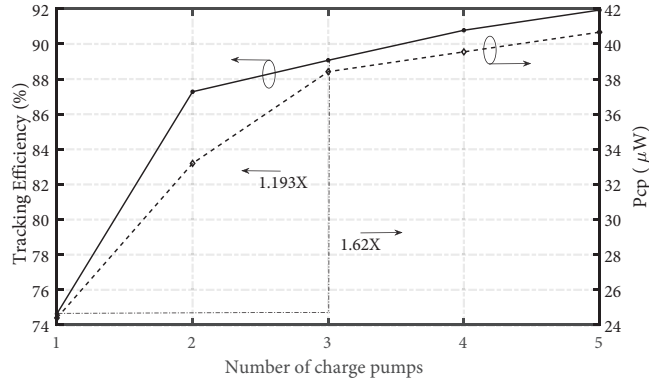**Figure 10**. The input voltage of the proposed converter under varying number of charge pumps.

Figure 11. Measured tracking efficiency and stored energy at Vcp under varying number of charge pumps.

It can be seen from Figure 11 that tracking efficiency and the stored power increase nonlinearly with a varying number of pumps. The proposed power extraction unit with five charge pumps improves the tracking efficiency by 123% as compared to one charge pump. Moreover, the proposed design achieves 66.7% more power extraction from the energy sources.
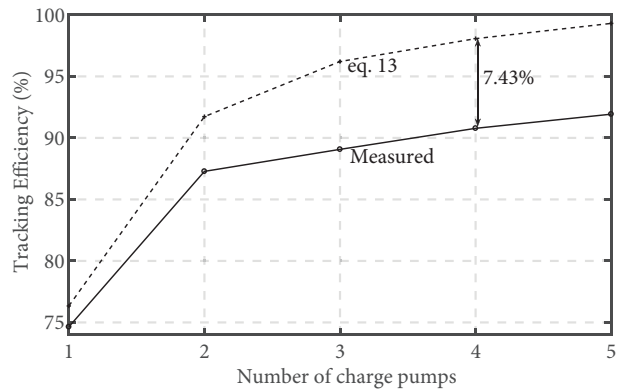

Figure 12. Measured and calculated (13) tracking efficiencies versus number of charge pumps.

By varying the number of pumps, the tracking efficiency calculated by (13) was plotted in Figure 12 (shown by the dashed line). The result for measured tracking efficiency from Figure 11 is also plotted (solid

line) for comparison. As shown, calculated tracking efficiency is higher than the measured one and the maximum disparity between the two curves is 7.43%. This is mainly due to the fact that, instead of (8b), (10) is used for the equivalent impedance. The frequency ratio of $f(1)/f(n)$ in (8b) is assumed to be equal to 1, but according to Figure 3 it is greater than 1. The reason for assuming the ratio as 1 is for simplicity and since the system parameters and oscillator structure for S-882 charge pump are not disclosed by the foundry. The (10) is nevertheless valid for showing a clear improvement on power extraction from energy source with the proposed design.
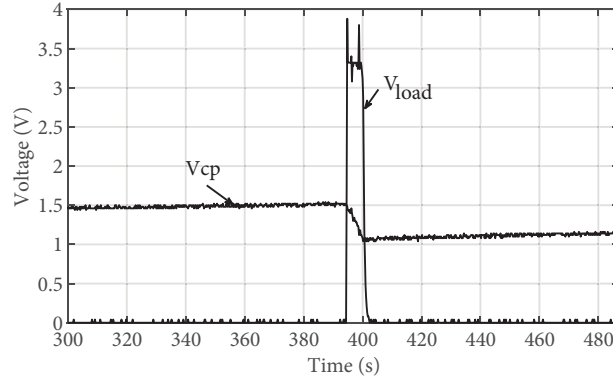

Figure 13. Measured waveforms of voltages at Vcp and V$_{load}$.

For demonstration purposes, a resistive load of 10 kΩ was connected to the output of the proposed converter. Measured voltages at Vcp and V$_{load}$ are shown in Figure 13. Once the voltage of the shared-capacitor reaches its discharge start voltage (V$_d$ = 1.5 V), the switch Mp is turned on and the boost converter is engaged to the shared-capacitor. Thus, the stored energy is transferred to the boost converter and the load voltage jumps to 3.3 V. Once the voltage at Vcp discharge to the charge start voltage (V$_c$ = 1.06 V), the transistor is cut off. Therefore, the boost converter is disengaged from the shared-capacitor and the load voltage drops from 3.3V to 0V. Powering load process is periodically repeated over time. For Figure 13, it takes roughly 392 s for the shared-capacitor to charge from V$_c$ to V$_d$ while the load active time is 8 s. These times can be adjusted with the changes in the capacitance of the shared-capacitor. However, the end-to-end efficiency (see (15)), which is the ratio of the power obtained at the load to the maximum power available from the energy source, varies for the proposed converter with 1 to 5 charge pumps, as shown in Figure 14. This indicates that the proposed converter improves the end-to-end efficiency by 133.2%–166.7% as compared to a one-charge-pump implementation. Transferring more energy to the load is achieved at the proposed converter because more energy is extracted from the energy source.

$$\eta_{end} = \eta_{track} \times \eta_1 \times \eta_2 = \frac{P_{in}}{P_{max}} \times \frac{P_{cp}}{P_{in}} \times \frac{P_{out}}{P_{cp}} = \frac{P_{out}}{P_{max}}, \tag{15}$$

where η_{track} is the tracking efficiency, η_1 and η_2 are the efficiencies of the first-stage and the second-stage converters, respectively.

Table 2 compares the existing works on power converters for energy sources. Among discrete component-based power converters, the proposed power converter achieved the highest end-to-end efficiency with maximum power point implementation. However, the design in [11], which was implemented in a 0.18 μm CMOS process and which required an external power supply, presents the highest efficiency. Thanks to an integrated circuit
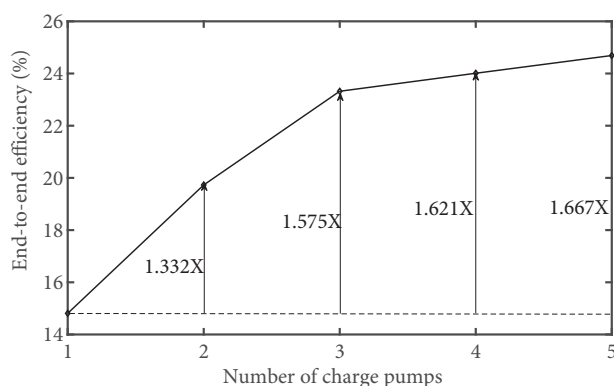
Figure 14. End-to-end efficiency of proposed two-stage power converter under varying number of charge pumps.

Table 2. Summary of the measured results.

Parameters	[7]	[11]	[17]	[19]	This work
Energy source	Multianode MFC	MFC TEG	MFC	MFC	Solar, TEG MFC
Output voltage	3.3 V	1.6 V–2 V	3.3 V	3.3 V	3.3 V
Min. input voltage	0.3 V	0.3 V	0.3 V	0.18 V	0.3 V
Max. available power	NA	11.2 μW ‡ 1.6 mW±	1 mW	NA	140 μW
MPPT	No	Yes	No	No	Yes
Efficiency	35.02%∗	32.14% ‡ † ∗ 62.5% ± † ∗	9.5% †	<9.5%†	24.69%
Topology	Charge pump Boost converter	Charge pump	Charge pump Boost converter	Transformer	Charge pump Boost converter
Technology	Discrete	0.18 μm	Discrete	Discrete	Discrete

∗ Not end-to-end. † Calculated based on the data in the paper. ‡MFC-low. ±MFC-high. ⋆ Required external supply.

implementation to allow the application-specific IC power converter design to achieve more efficiency than discrete ones. In addition, the target output voltage of the converter in [11] (i.e. 2 V) is far from other ones (e.g., 3.3 V). To the best of the author's knowledge, the design in [11] would require either a second-stage converter or an increase in the number of pumping stages to reach the target output voltage of 3.3 V. This results in a decrease at the end-to-end efficiency. For low-power energy sources, an efficient custom integrated solution to implement the proposed circuit will provide more efficiency than the current design.

6. Conclusion

This paper presents a power converter design with maximum power point for various energy sources, both experimentally and numerically are analyzed. Maximum power extraction from energy sources is obtained through n number of charge pumps connected in parallel in the first stage converter. The tracking efficiency is enhanced by 117%–123% as compared to the one-charge-pump implementation in the first stage converter.

Proposed power converter provides 66.7% more power extracted from the energy source than the single charge pump one. The proposed inductorless power converter enhances the end-to-end efficiency by $1.67\,X$ as compared to one charge pump implementation. The proposed power converter maximizes power extraction not only from low power energy sources but also from high power energy sources.

References

[1] Huang G, Umaz R, Karra U, Li B, Wang L. A biomass-based marine sediment energy harvesting system. In: International Symposium on Low Power Electronics and Design (ISLPED); Beijing, China; 2013. pp. 359-364.

[2] Karra U, Muto E, Umaz R, Kolln M, Santoro C et al. Performance evaluation of activated carbon-based electrodes with novel power management system for long-term benthic microbial fuel cells. International Journal of Hydrogen Energy 2014; 39(36): 21847-21856.

[3] Chew KWR, Sun Z, Tang H, Siek L. A 400 nW single-inductor dual-input-tri-output dc-dc buck-boost converter with maximum power point tracking for indoor photovoltaic energy harvesting. In: IEEE International Solid-State Circuits Conference Digest of Technical Papers; San Francisco, USA; 2013. pp. 68-69.

[4] Das A, Gao Y, Kim TTH. A 220-mv power-on-reset based self-starter with 2-nW quiescent power for thermoelectric energy harvesting systems. IEEE Transactions on Circuits and Systems I: Regular Papers 2017; 64(1): 217-226.

[5] Dini M, Romani A, Filippi M, Tartagni M. A nanocurrent power management ic for low-voltage energy harvesting sources. IEEE Transactions on Power Electronics 2016; 31(6): 4292-4304.

[6] Mansano A, Bagga S, Serdijn W. A high efficiency orthogonally switching passive charge pump rectifier for energy harvesters. IEEE Transactions on Circuits and Systems I: Regular Papers 2013; 60(7): 1959-1966.

[7] Umaz R, Garrett C, Qian F, Li B, Wang L. A power management system for multianode benthic microbial fuel cells. IEEE Transactions on Power Electronics 2017; 32(5): 3562-3570.

[8] Qiu Y, Van Liempd C, het Veld BO, Blanken PG, Van Hoof C. $5\,\mu$W-to-10mW input power range inductive boost converter for indoor photovoltaic energy harvesting with integrated maximum power point tracking algorithm. In: IEEE International Solid-State Circuits Conference; San Francisco, USA; 2011. pp. 118-120.

[9] Huang G, Umaz R, Karra U, Li B, Wang L. A power management integrated system for biomass-based marine sediment energy harvesting. International Journal of High Speed Electronics and Systems 2014; 23: 1450012 (1-20).

[10] Umaz R, Wang L. Design of an inductorless power converter with maximizing power extraction for energy harvesting. International Journal of High Speed Electronics and Systems 2018; 27(01n02): 1840007.

[11] Carreon-Bautista S, Erbay C, Han A, Sanchez-Sinencio E. An inductorless dc-dc converter for an energy aware power management unit aimed at microbial fuel cell arrays. IEEE Journal of Emerging and Selected Topics in Power Electronics 2015; 3(4): 1109-1121.

[12] Shih YC, Otis BP. An inductorless dc-dc converter for energy harvesting with a 1.2- μw bandgap-referenced output controller. IEEE Transactions on Circuits and Systems II: Express Briefs 2011; 58(12): 832-836.

[13] Umaz R, Wang L. An energy combiner design for multiple microbial energy harvesting sources. In: Proceedings of the on Great Lakes Symposium on VLSI; Alberta, CA; 2017. pp. 443-446.

[14] Tanzawa T, Tanaka T. A dynamic analysis of the dickson charge pump circuit. IEEE Journal of Solid-State Circuits 1997; 32(8): 1231-1240.

[15] Dickson JF. On-chip high-voltage generation in mnos integrated circuits using an improved voltage multiplier technique. IEEE Journal of Solid-State Circuits 1976; 11(3): 374-378.

[16] Seiko Instruments Inc. Ultra low voltage operation charge pump IC for step UP DC-DC converter startup. S882Z Datasheet 2010.

[17] Meehan A, Gao H, Lewandowski Z. Energy harvesting with microbial fuel cell and power management system. IEEE Transactions on Power Electronics 2011; 26(1): 176-181.

[18] STMicroelectronics. Synchronous rectifier step up converter. L6920DB Datasheet Oct. 2006.

[19] Yang F, Zhang D, Shimotori T, Wang K, Huang Y. Study of transformer-based power management system and its performance optimization for microbial fuel cells. Journal of Power Sources 2012; 205: 86-92.